SCIENCE CHINA
Information Sciences

• RESEARCH PAPER •

June 2026, Vol. 69, Iss. 6, 162502:1–162502:9
https://doi.org/10.1007/s11432-025-4611-8

Link optimization of duplex quantum communication systems

Peng-Hao NIU[1], Fei-Hao ZHANG[1], Rui-Song BAO[2] & Gui-Lu LONG[1,2,3,4*]

[1]*Beijing Academy of Quantum Information Sciences, Beijing 100193, China*
[2]*State Key Laboratory of Low-dimensional Quantum Physics and Department of Physics, Tsinghua University, Beijing 100084, China*
[3]*Frontier Science Center for Quantum Information, Beijing 100084, China*
[4]*Beijing National Research Center for Information Science and Technology, Beijing 100084, China*

Received 6 May 2025/Revised 31 July 2025/Accepted 18 September 2025/Published online 27 April 2026

Abstract Quantum communication provides us with a novel means of secure information transmission. Concurrently, there is a growing demand for multi-user quantum networks in tandem with the development of quantum communication devices. Given that most terrestrial quantum networks rely on optical fibers, the escalating user demand has rendered the cost and complexity of multi-fiber links critical issues that demand immediate attention. This article presents a duplex quantum communication link optimization scheme. This scheme significantly reduces the consumption of fiber link resources in duplex quantum communication systems, simplifies the deployment process, and cuts down costs. Based on this scheme, a corresponding experimental system was constructed and tested. The test results demonstrate that the scheme effectively simplifies the link without significantly compromising the performance of the original system.

Keywords quantum communication, quantum network, link optimization

Citation Niu P-H, Zhang F-H, Bao R-S, et al. Link optimization of duplex quantum communication systems. Sci China Inf Sci, 2026, 69(6): 162502, https://doi.org/10.1007/s11432-025-4611-8

1 Introduction

Quantum cryptography provides a secure means of information transmission based on the principles of quantum physics, diverging from traditional computational security approaches. Leveraging these quantum physical principles, numerous protocols have been developed [1–4], among which quantum secure direct communication (QSDC) stands out. The QSDC protocol was first proposed in 2000 [3]. Subsequently, several related protocols were developed, and their security was proven [5–20]. After some proof-of-principle experiments [21–23], the world's first QSDC prototype was developed in 2019 [24]. Then, the communication distance was further extended to over 100 km [25]. In 2025, unidirectional QSDC was proposed, and the corresponding practical system was completed, achieving a communication rate of 2.38 kbps over 104.8 km of optical fiber [26]. Moreover, research on QSDC and related quantum networks is continuously progressing [27–37].

The existing QSDC terminal system architecture is composed of a transmitter and a receiver, which enables point-to-point unidirectional secure information transmission [38]. Nevertheless, in practical communication applications, participants not only need to send messages but also must be able to receive messages simultaneously. Duplex communication, for example, in secure telephone applications, represents a common requirement. When implementing duplex communication, each communication node has to deploy both a transmitter and a receiver. Under the current circumstances, a point-to-point duplex QSDC system needs six separate fiber links to complete the secure communication process [38]. As a result, the demand for fiber resources is significant, particularly in long-distance communication scenarios, which leads to high deployment and maintenance costs [39].

In practice, multi-node communication represents a far more prevalent application scenario. It necessitates the utilization of QSDC terminals to establish networks, thereby fulfilling the secure communication requirements of multiple users [40]. In such circumstances, the existing duplex QSDC systems face a significant challenge. As the number of network nodes expands, these systems become increasingly complex in terms of network hardware due

* Corresponding author (email: gllong@tsinghua.edu.cn)

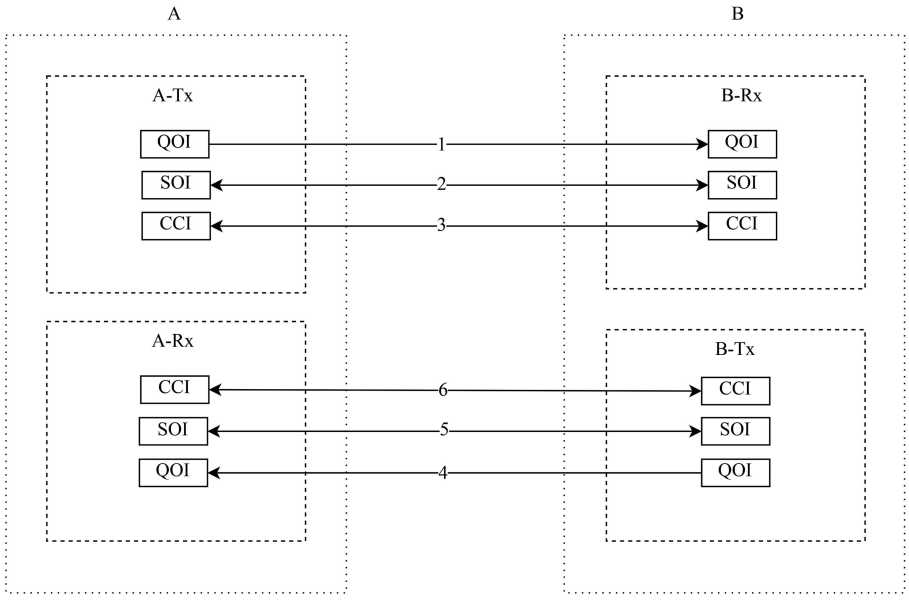

Figure 1 The optical links of the conventional D-Q system. Tx: transmitter; Rx: receiver; QOI: quantum optical interface; SOI: synchronization optical interface; CCI: classical communication interface.

to their heavy dependence on a multitude of fiber optic links. Consequently, the link-switching process becomes arduous when handling service requests, giving rise to elevated operating costs and potential stability issues [41].

A practical way is to optimize the links of a duplex QSDC system, allowing multiple fiber channels to be multiplexed and coexist within a single fiber, which remarkably decreases the number of fiber links needed for duplex communication. As a result, the deployment process is simplified, and the overall construction and maintenance expenses of QSDC networks are reduced.

In this study, we propose a novel scheme for constructing a duplex QSDC system. This innovative approach significantly streamlines the fiber link infrastructure, reducing the six links required in a traditional point-to-point QSDC system to just two. To validate the feasibility of our proposed scheme, we developed and experimentally tested a corresponding system. The experimental results show that our scheme achieves substantial link simplification while maintaining negligible degradation to the original system's performance, thereby highlighting its considerable potential for practical applications.

2 Design of the woven duplex QSDC system

To illustrate our proposed design, we first examine the fiber optic link structure of the existing duplex QSDC (denoted as D-Q) system, as depicted in Figure 1. At nodes A and B, each node is equipped with two terminals: a transmitter and a receiver, enabling duplex communication. Each terminal features three physical interfaces for connecting to fiber links. The quantum optical interface (QOI) is connected to the unidirectional link and serves to transmit quantum signals from the transmitter to the receiver (links 1 and 4). The synchronization optical interface (SOI) is tasked with time synchronization between the terminals (links 2 and 5), whereas the classical communication interface (CCI) facilitates the classical exchange of information between the terminals (links 3 and 6).

The QOI uses an FC physical interface, while CCI communicates based on the Ethernet protocol and utilizes a small form-factor pluggable (SFP) transceiver module for optical signal transmission. The SOI also uses SFP transceiver modules to convert optical synchronization signals into electrical signals. These signals are processed by FPGA-based clock data recovery (CDR) circuits, including the phase-locked loop (PPL), which lock onto the incoming signal's frequency and phase while handling transmission-induced noise, ultimately achieving a hundred-picosecond time synchronization accuracy.

It is evident that the existing D-Q system necessitates six fiber links. While this is viable in point-to-point environments, real network deployments may pose challenges due to the often limited availability of fiber resources, particularly in multi-node network scenarios. To tackle this problem, we have devised a novel link scheme that substantially reduces the number of fiber links required by the D-Q system, as illustrated in Figure 2.

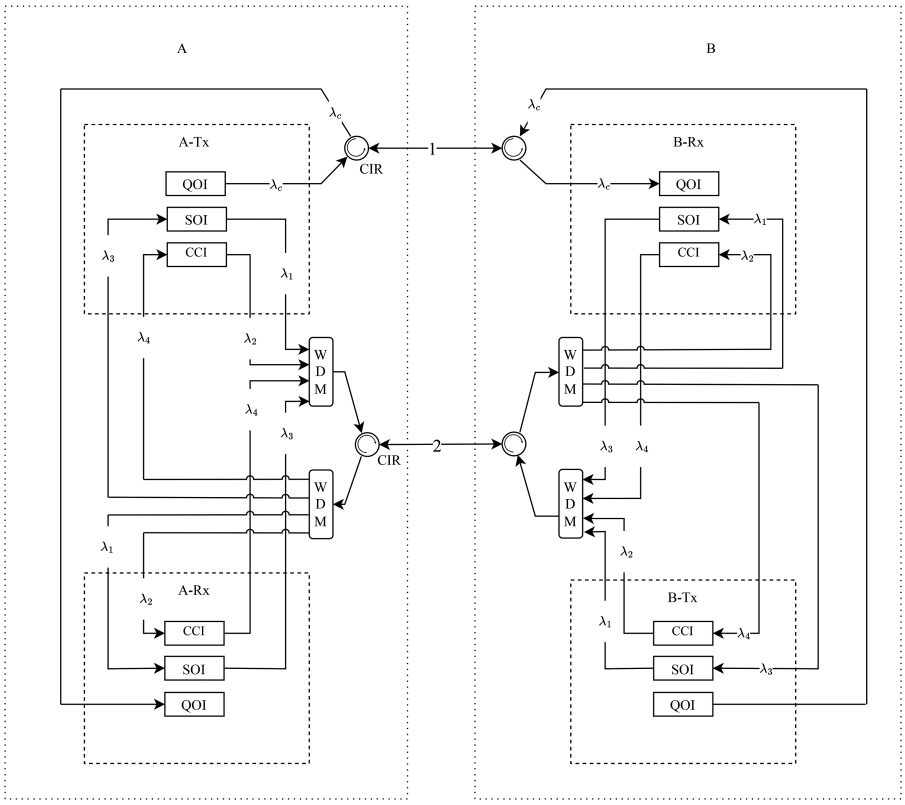

Figure 2 The link optimization scheme of the D-Q system, which forms the W-Q system. CIR: optical circulator, WDM: wavelength division multiplexing.

We divide all the link signals of the D-Q system into two categories: one for quantum optical signals and the other for classical optical signals. Then, we couple these signals into two separate optical fiber links (links 1 and 2 in Figure 2) to prevent classical optical signals from interfering with quantum optical signals. Since the quantum signal is a unidirectional optical signal traveling from Tx to Rx, we employ a circulator (CIR) to connect the QOI signals of the four terminals, forming the single transmission link 1.

Regarding classical signals, each terminal is equipped with an SOI and a CCI. Both use SFP optical transceivers, which are capable of handling both incoming and outgoing signals. Consequently, at one node, there will be eight classical signals with different directions (four outward and four inward). As shown in Figure 2, we use a combination of WDM and CIR to couple all classical signals between two nodes into a single link. WDM technology streamlines the utilization of links within a communication system [42–44]. Four different wavelengths are utilized to implement this design. We refer to the D-Q system with the link optimization scheme, which has intertwined optical paths in the nodes, as the woven duplex QSDC system, abbreviated as W-Q.

3 Experimental validation of the woven duplex QSDC system

Based on the proposed scheme, we implemented a point-to-point D-Q system for experimental validation. The system employs phase encoding and utilizes a 50 km single-mode fiber as the quantum channel. For wavelength selection, the quantum signal operates at $\lambda_c = 1550$ nm, while the wavelengths for classical signals are set as $\lambda_1 = 1530$ nm, $\lambda_2 = 1590$ nm, $\lambda_3 = 1510$ nm, and $\lambda_4 = 1570$ nm, as illustrated in Figure 2. The consideration for choosing these wavelengths is that the operating wavelength of quantum signals is 1550 nm, as determined by the optical module of the quantum communication system. For classical signals, since both classical and quantum signals are transmitted through the same type of single-mode optical fiber, we select different wavelengths at 20 nm intervals centered on 1550 nm, with reference to the ITU-T G.694.2 standard. The channel spacing of 20 nm provides sufficient bandwidth for protection between adjacent channels. The WDM device employs 60 dB of isolation to ensure the signal has a sufficient signal-to-noise ratio at the receiver interface, thereby suppressing potential crosstalk that may come from co-fiber transmission. The system's repetition frequency is 1.25 GHz. Considering that the quantum pulse arrival time, phase modulation time, and single-photon detector gating time need to be accurately aligned,

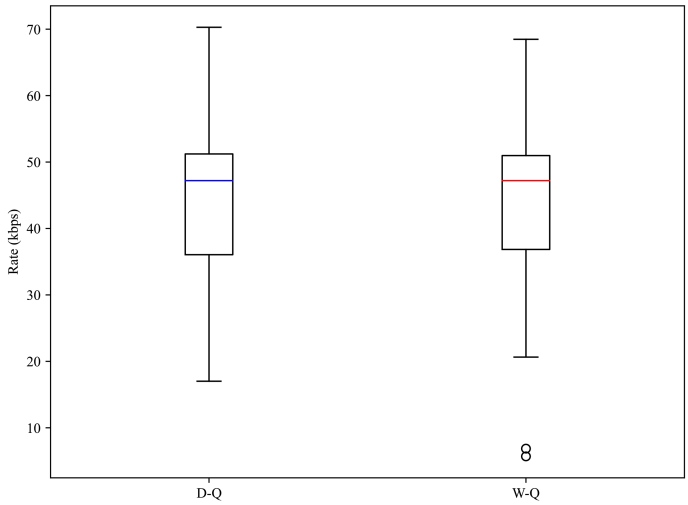

Figure 3 (Color online) Box plots of the transmission rate data sets for the D-Q and W-Q systems. The blue horizontal line and the red horizontal line represent the median of the respective samples, and the top and bottom edges of the box represent the upper quartile and lower quartile, respectively.

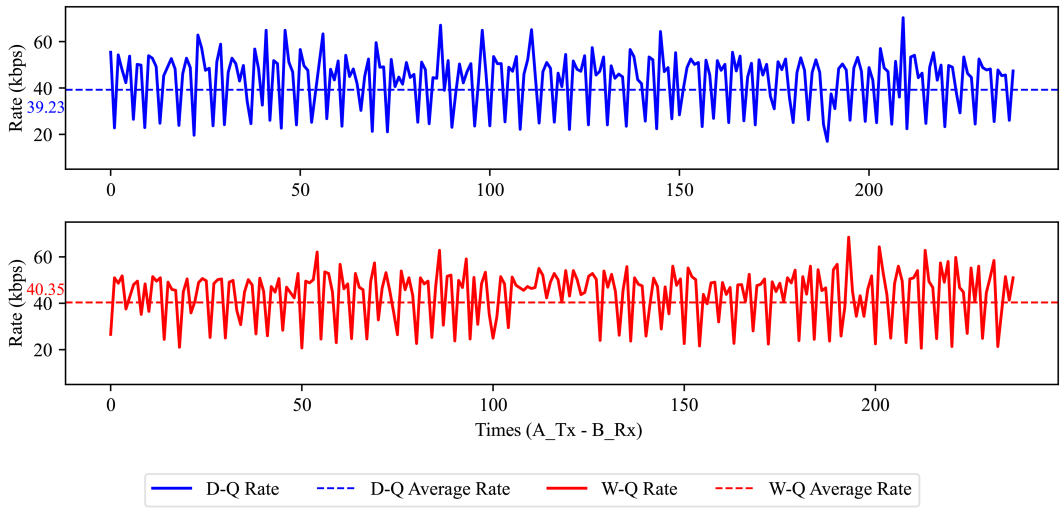

Figure 4 (Color online) Transmission rate of the D-Q and W-Q systems, from A-Tx to B-Rx. The dashed line represents the average transmission rate.

which requires high accuracy of time synchronization, the selection of the above-mentioned optical parameters will effectively support the stable transmission of synchronization and classical signals.

Subsequently, we conducted a transmission experiment on the system. We used fixed-size data packets (15.912 kB) and repeatedly transmitted them. The transmission time of each packet was recorded to calculate its corresponding transmission rate. By testing both the D-Q and W-Q systems, we collected approximately 240 data points for each system, where each point corresponds to a transmission rate from A-Tx to B-Rx, as depicted in Figure 2. The box plots of the two data sets are presented in Figure 3. From these box plots, we can clearly observe the distribution characteristics and potential differences in the transmission rates of the two systems, which provide a solid foundation for further comparative analysis and evaluation of the performance of the D-Q and W-Q systems.

Figure 4 illustrates the transmission rates of both systems after outliers have been removed from the data. In each sub-figure, the dashed line represents the average transmission rate of D-Q and W-Q, respectively. It is important to note that the values of the dashed lines do not denote the arithmetic mean of the transmission data set; instead, they are calculated by dividing the total size of all packets in the data set by the total transmission time.

We will utilize the quantum bit error rate (QBER) to assess the consistency of transmission rate fluctuations in the D-Q and W-Q systems. In QSDC systems, the QBER can significantly affect the secure transmission rate, as reported in the study by Pan et al. [26]. Therefore, to ensure a fair comparison, the transmission rate performance of the systems should be evaluated under similar QBER conditions.

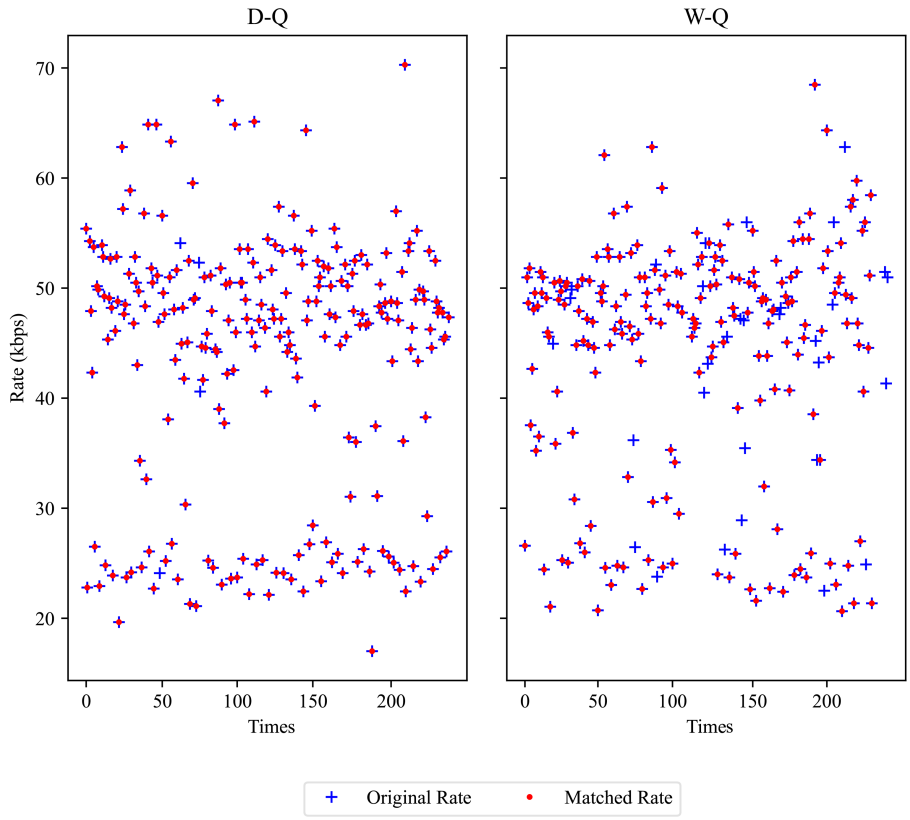

Figure 5 (Color online) Matching effect verification of transmission rate for the D-Q and W-Q systems.

In our experimental setup, distinct programs were employed to conduct data packet transmission tests and QBER measurements. A single data packet transmission took approximately 0.4 s on average, whereas real-time QBER acquisition required about 1 s. This disparity in time scales led to a situation where, for a set of nearly 240 real-time rate data points, the corresponding QBER data amounted to less than 100. To address this issue, we devised a matching procedure.

First, we recorded the timestamps of the start and completion of each packet's transmission. Using the start-transmission timestamp as a reference, we matched the QBER acquisition timestamps within a range of plus or minus 600 ms to obtain the corresponding QBERs for all rate data. Rate data that could not be matched were discarded. To evaluate the impact of this data discarding process, Figure 5 presents a comparison between the original rate data (excluding outliers) and the rate data after QBER matching. The cross symbols denote the original rate data, while the red dots represent the matched rate data.

Notably, the data measured under the D-Q and W-Q systems retained a substantial number of original data points after the matching process. Specifically, 98.33% of the data remained in the D-Q system, and 86.81% remained in the W-Q system. Additionally, we analyzed the time differences between the respective timestamps of the rate and QBER for each matched pair. The results showed that the average time difference for the D-Q system was 9 ms, and for the W-Q system, it was 15 ms. These minor time differences indicate that, after matching, the QBER values associated with each rate data point are temporally close and can effectively represent the actual QBER values of the corresponding systems during transmission.

Now, we have obtained the transmission rates for the D-Q and W-Q systems, along with the QBER corresponding to the transmission process at each rate. Figure 6 illustrates the distribution of the transmission rate of the D-Q system with respect to QBER. It should be noted that the D-Q system used for the experimental validation of our scheme is based on the STIKE protocol proposed in [26]. According to this protocol, data packets are encrypted with a key of the desired length from a secure key sink before transmission. The change in QBER will change the length of the newly generated key, but it will not affect the existing key in the sink. Therefore, the transmission rate does not show a significant downward trend as the QBER increases. However, the system has a real-time compensation program to handle QBER variations, which is a frequent and rapid process. This process will temporarily occupy part of the transmission time, leading to the fluctuation of the transmission rate. Consequently, the fluctuation

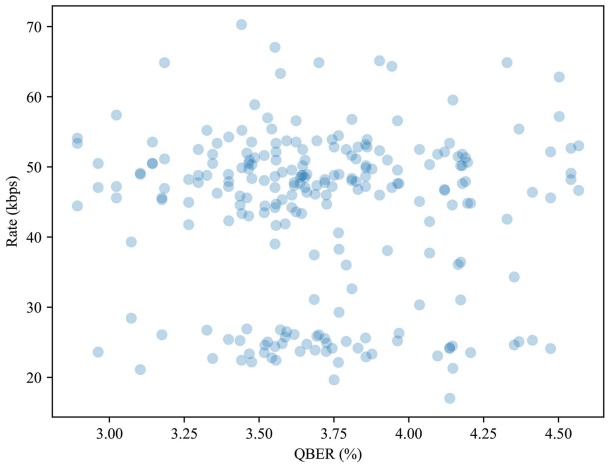

Figure 6 (Color online) D-Q system transmission rate distribution under QBER.

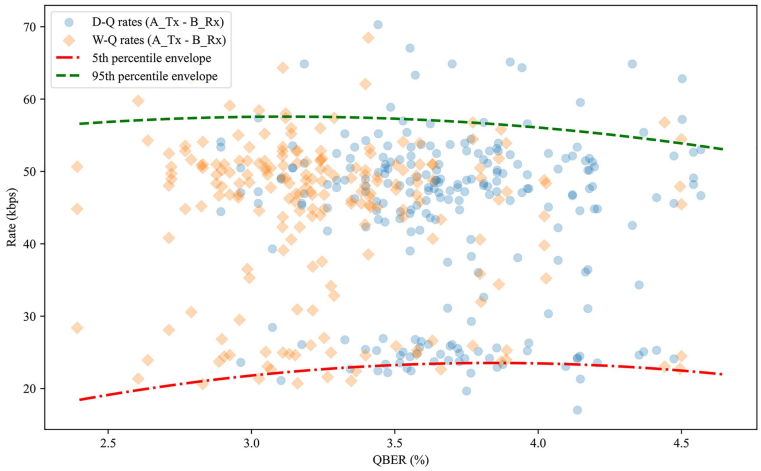

Figure 7 (Color online) Envelope of D-Q system transmission rates and W-Q system's transmission rates distribution, from A-Tx to B-Rx.

of the transmission rate under different QBER reflects the current operating status of the system, and we need to investigate further the impact of the link optimization scheme on the D-Q system.

Next, the rate history fluctuation envelope of the D-Q system needs to be determined. The QBER values are categorized into three groups: 3%–3.5%, 3.5%–4.0%, and 4.0%–4.5%. The 5th and 95th percentiles of the corresponding rates for each QBER group are calculated separately. These percentiles are then used to fit the 5th and 95th envelopes of the rate fluctuations of the D-Q system.

Based on this envelope, the proportion of the D-Q system's transmission rate that exceeds the historical envelope during the overall fluctuation process can be calculated. Subsequently, taking this envelope as a benchmark, the proportion of the W-Q system's transmission rate that exceeds the envelope during the QBER-related fluctuation process is computed.

As illustrated in Figure 7, this figure presents the transmission rate fluctuation envelope of the D-Q system and the distribution of the W-Q system's transmission rate within the same envelope. The analysis reveals that 11.91% of the D-Q system's transmission rate data points exceed the envelope during fluctuations. In contrast, within the same envelope, 8.82% of the W-Q system's rate values exceed the envelope. This indicates that, after implementing the link optimization scheme on the D-Q system, the fluctuation of its transmission rate remains within the original level. In other words, the link optimization scheme has a negligible impact on the original QSDC system.

Following the same methodology, we also tested the transmission rates from B-Tx to A-Rx for both D-Q and W-Q systems, as shown in Figures 8 and 9. The test data indicate that, for the transmission from B-Tx to A-Rx, 10.12% of the transmission rate data points exceed the envelope of the D-Q system, while for the W-Q system, this proportion is 3.28%. These results further support our previous findings.

In the practical experiment of the scheme shown in Figure 2, we discovered that back reflections occur when merging fiber-optic links. This phenomenon arises because the input wavelengths at certain physical interfaces

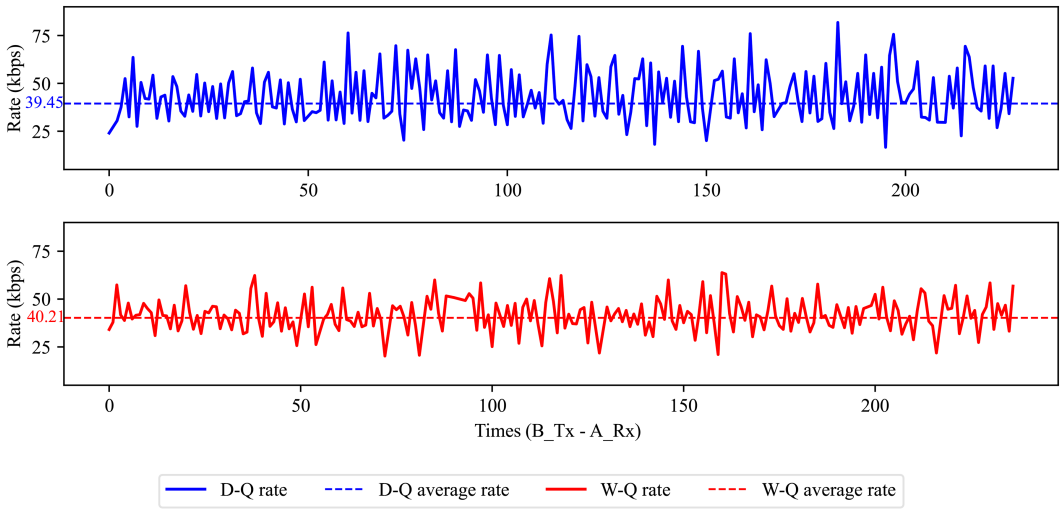

Figure 8 (Color online) Transmission rates of the D-Q and W-Q systems, from B-Tx to A-Rx. The dashed line represents the average transmission rate.

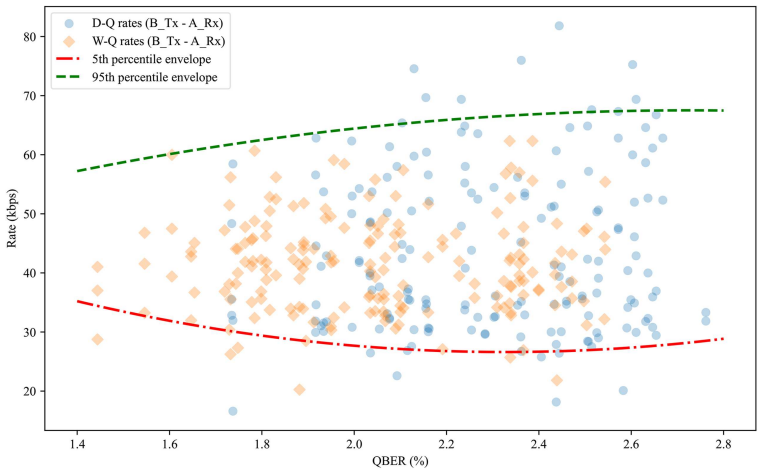

Figure 9 (Color online) Envelope of D-Q system transmission rates and W-Q system's transmission rates distribution, from B-Tx to A-Rx.

match the output wavelengths of other interfaces. These reflections can potentially disrupt the signal transmission between terminals. To address this issue, we incorporated fiber optic isolators and replaced the fiber optic connectors with FC/APC interfaces, which effectively suppressed the back reflections.

4 Conclusion

In this paper, we propose a link optimization scheme for quantum communication duplex systems. This scheme primarily leverages common, proven fiber optic components. We implemented the scheme on a QSDC system, which reduces the number of fiber optic links from the original six to just two. This significant reduction not only cuts down the deployment cost of a duplex QSDC system but also decreases the system's complexity and maintenance expenses during network construction.

We conducted tests on the transmission rates of both the original duplex QSDC system and the system with the proposed scheme applied. The results showed that the performance of the two systems was comparable. Through an analysis of the fluctuation relationship between the transmission rate and the QBER, we determined that the rate fluctuation of the QSDC system adopting our scheme did not exceed the fluctuation range of the original system. Consequently, we conclude that the proposed scheme enhances the existing system without causing significant negative impacts on its performance. Moreover, the scheme has been verified through tests in real-world systems, demonstrating its potential application value.

As mentioned in the previous section, the time alignment of individual operations in a quantum communication

system is demanding, so the accuracy and stability of time synchronization are crucial. Our experimental system can achieve time synchronization accuracy at the hundred picosecond level, which meets the system's 1.25 GHz repetition frequency requirement. Tests of the link optimization scheme show that the scheme can guarantee the time synchronization accuracy required for the regular operation of the system, demonstrating the scheme's robustness. Future work could explore how different signal power levels, fiber conditions, and potential nonlinear optical effects influence signal transmission stability to further quantify the performance boundaries of our scheme.

Additionally, when implementing the proposed scheme in practical scenarios, the issue of back reflection should be taken into account. This problem can be addressed by introducing unidirectional fiber optic devices and changing the type of fiber optic connectors. Furthermore, a more advanced solution could be to optimize the wavelength selection of the scheme to avoid the back reflection problem altogether.

Although our proposed scheme separates quantum and classical signals to mitigate the potential impact of nonlinear effects, from an architectural perspective, it is feasible to couple all signals into a single optical fiber due to their utilization of different wavelengths. Notably, the scheme is scalable and can support a greater number of wavelengths compared to the scenario presented in this paper. Nevertheless, the nonlinear effects and noise implications associated with the transmission of multiple wavelengths in optical fibers require further investigation.

Acknowledgements This work was supported by National Natural Science Foundation of China (Grant Nos. 62471046, 12204051).

References

1 Bennett C H, Brassard G. Quantum cryptography: public key distribution and coin tossing. In: Proceedings of the IEEE International Conference on Computers, Systems and Signal Processing, Bangalore, 1984. 175–179
2 Ekert A K. Quantum cryptography based on Bell's theorem. Phys Rev Lett, 1991, 67: 661–663
3 Long G L, Liu X S. Theoretical efficient high capacity quantum key distribution scheme. ArXiv:quant-ph/0012056
4 Long G L, Liu X S. Theoretically efficient high-capacity quantum-key-distribution scheme. Phys Rev A, 2002, 65: 032302
5 Deng F G, Long G L, Liu X S. Two-step quantum direct communication protocol using the Einstein-Podolsky-Rosen pair block. Phys Rev A, 2003, 68: 042317
6 Deng F G, Long G L. Secure direct communication with a quantum one-time pad. Phys Rev A, 2004, 69: 052319
7 Wen K, Deng F G, Long G L. Reusable Vernam cipher with quantum media. ArXiv:0711.1632
8 Bennett C H, Brassard G, Breidbart S. Quantum cryptography II: how to re-use a one-time pad safely even if P=NP. Nat Comput, 2014, 13: 453–458
9 Niu P H, Zhou Z R, Lin Z S, et al. Measurement-device-independent quantum communication without encryption. Sci Bull, 2018, 63: 1345–1350
10 Zhou L, Sheng Y B, Long G L. Device-independent quantum secure direct communication against collective attacks. Sci Bull, 2019, 65: 12–20
11 Wu J, Lin Z, Yin L, et al. Security of quantum secure direct communication based on Wyner's wiretap channel theory. Quantum Engineering, 2019, 1: e26
12 Niu P H, Wu J W, Yin L G, et al. Security analysis of measurement-device-independent quantum secure direct communication. Quantum Inf Process, 2020, 19: 356
13 Sheng Y B, Zhou L, Long G L. One-step quantum secure direct communication. Sci Bull, 2022, 67: 367–374
14 Zhou L, Xu B W, Zhong W, et al. Device-independent quantum secure direct communication with single-photon sources. Phys Rev Appl, 2023, 19: 014036
15 Cao Z, Lu Y, Chai G, et al. Realization of quantum secure direct communication with continuous variable. Research, 2023, 6: 0193
16 Cao Z, Liang Z, Zhang Y, et al. Atmospheric continuous-variable quantum secure direct communication with orbital angular momentum multiplexing. J Opt Soc Am B, 2024, 41: 2328–2339
17 Zeng H, Du M M, Zhong W, et al. High-capacity device-independent quantum secure direct communication based on hyper-encoding. Fundamental Res, 2024, 4: 851–857
18 Liu C, Zhang C, Gu S P, et al. Receiver-device-independent quantum secure direct communication. Sci China-Phys Mech Astron, 2025, 68: 250311
19 Pan D, Long G L, Yin L, et al. The evolution of quantum secure direct communication: on the road to the qinternet. IEEE Commun Surv Tut, 2024
20 Cao Z W, Zhang Y J, Chai G, et al. Continuous-variable quantum secure direct communication based on N-APSK with Boltzmann-Maxwell distribution. Chin Phys B, 2025, 34: 030303
21 Hu J Y, Yu B, Jing M Y, et al. Experimental quantum secure direct communication with single photons. Light Sci Appl, 2016, 5: e16144
22 Zhang W, Ding D S, Sheng Y B, et al. Quantum secure direct communication with quantum memory. Phys Rev Lett, 2017, 118: 220501
23 Zhu F, Zhang W, Sheng Y, et al. Experimental long-distance quantum secure direct communication. Sci Bull, 2017, 62: 1519–1524
24 Qi R, Sun Z, Lin Z, et al. Implementation and security analysis of practical quantum secure direct communication. Light Sci Appl, 2019, 8: 22
25 Zhang H, Sun Z, Qi R, et al. Realization of quantum secure direct communication over 100 km fiber with time-bin and phase quantum states. Light Sci Appl, 2022, 11: 83
26 Pan D, Liu Y C, Niu P, et al. Simultaneous transmission of information and key exchange using the same photonic quantum states. Sci Adv, 2025, 11: eadt4627
27 Qi Z, Li Y, Huang Y, et al. A 15-user quantum secure direct communication network. Light Sci Appl, 2021, 10: 183
28 Huang J, Chen X, Li X, et al. Chip-based photonic graph states. AAPPS Bull, 2023, 33: 14
29 Ying J W, Zhao P, Zhong W, et al. Passive decoy-state quantum secure direct communication with a heralded single-photon source. Phys Rev Appl, 2024, 22: 024040
30 Wang M, Long G L. Lattice-based access authentication scheme for quantum communication networks. Sci China Inf Sci, 2024, 67: 222501
31 Lu Q H, Wang F X, Chen W, et al. Quantum key distribution over a mimicked dynamic-scattering channel. Sci China Inf Sci, 2024, 67: 142503
32 Ying J W, Wang J Y, Xiao Y X, et al. Passive-state preparation for quantum secure direct communication. Sci China-Phys Mech Astron, 2025, 68: 240312
33 Sun Z Z, Cheng Y B, Wang M, et al. Quantum blockchain relying on quantum secure direct communication network. IEEE Internet Things J, 2025, 12: 14375–14385
34 Sun Z Z, Cheng Y B, Ruan D, et al. Quantum communication network routing with circuit and packet switching strategies. IEEE J Sel Areas Commun, 2025, 43: 1887–1900

35 Ding C W, Wang W Y, Zhang W D, et al. Quantum secure direct communication based on quantum error correction code. Appl Phys Lett, 2025, 126: 024002
36 Yang Y, Li Y, Li H, et al. A 300-km fully-connected quantum secure direct communication network. Sci Bull, 2025, 70: 1445–1451
37 Zhang R M, Fan Y R, Yuan C Z, et al. Bridging quantum elementary links with spectral steering. Sci China Inf Sci, 2025, 68: 180505
38 Niu P H, Guo J X, Bao R S, et al. Quantum enhanced hazardous substances surveillance system. Quantum Eng, 2024, 2024: 1494088
39 Tsolaridis G, Fuchs S, Jehle A, et al. High speed, multi-channel, isolated data transmission with a single fiber based on intensity modulation. In: Proceedings of the 20th European Conference on Power Electronics and Applications, 2018
40 Niu P H, Zhang F H, Chen X W, et al. QNUS: reducing terminal resources in quantum secure direct communication network using switches. Quantum Eng, 2022, 2022: 1–6
41 Staley J, Muknahallipatna S, Johnson H. Fibre channel based storage area network modeling using OPNET for large fabric simulations: preliminary work. In: Proceedings of the 32nd IEEE Conference on Local Computer Networks (LCN 2007), 2007. 234–236
42 Ferreira A, Pérennes S, Rivano H, et al. Models, complexity and algorithms for the design of multi-fiber WDM networks. Telecommun Syst, 2003, 24: 123–138
43 Nomikos C, Pagourtzis A, Potika K, et al. Fiber cost reduction and wavelength minimization in multifiber WDM networks. In: Proceedings of Networking 2004. Berlin: Springer, 2004. 150–161
44 Gunasekaran P, Pazhani A A J, Rameshbabu A, et al. Role of wavelength division multiplexing in optical communication. In: Modeling and Optimization of Optical Communication Networks. Hoboken: John Wiley & Sons, Ltd., 2023. 217–234